

Electromagnetic Structure of the Giant Resonance in Oxygen-16†

F. H. LEWIS, JR.

Institute of Theoretical Physics, Department of Physics, Stanford University, Stanford, California

(Received 5 December 1963)

The transverse inelastic form factor for excitation of the giant resonance in oxygen-16 is calculated by means of the particle-hole theory of the giant resonance. The calculation is done in such a way that no free parameters are involved. In addition, calculations similar to those of Brown, Castillejo, and Evans have been carried out and the form factor has also been calculated for the Goldhaber-Teller model. The results are compared with 180° electron-scattering experiments and with photoabsorption data. It is found that the particle-hole calculations predict the observed behavior for the squared form factor, and also the change in the shape of the giant resonance cross section which is seen experimentally as the momentum transfer q is varied. Neither of these effects is predicted by the Goldhaber-Teller model. Numerical results are presented for all of the different theoretical models, and it is found that the calculations involving no free parameters predict essentially the observed energy levels for the giant resonance and yield form factors which are consistent with all of the experiments considered.

I. INTRODUCTION

DURING the past few years a great deal of experimental and theoretical work has been devoted to the determination of the structure of the nuclear giant dipole resonance. While the earlier descriptions of this effect were formulated in terms of collective models of nuclear motion,^{1,2} the experimental observations of splittings^{3,4} in the resonance have generally provided encouragement for more detailed calculations in terms of single-particle models.⁵ Some of the more successful calculations of this type have been done by Elliott and Flowers⁶ and Brown^{7,8} and co-workers. These authors have both formulated theories for the giant resonance in which a two-particle interaction is used to generate configuration mixing among a set of single-particle shell-model states. These calculations are able to predict fairly successfully the energies of the states making up the giant resonance and the distribution of dipole strength among these states as observed in photoabsorption and (p,γ) experiments.⁹

One of the most valuable experimental techniques for studying nuclear structure is inelastic electron scattering.¹⁰⁻¹³ In a previous paper¹⁴ the transverse

inelastic form factor for electromagnetic excitation of the giant resonance was discussed and calculated in terms of several different theoretical models of the giant resonance, and the results were compared with experimental data from inelastic electron scattering at 180° and from photoabsorption experiments for the case of carbon 12. It was shown there that the form factors measured in electron scattering provide a much more sensitive test of any theory of the giant resonance than does just the photoabsorption and (p,γ) data alone. The particle-hole theory of Brown⁸ was seen to be mainly in agreement with the experiments, while the collective motion models of the giant resonance gave completely wrong form factors. By making more detailed comparisons of theory with experiment it was even possible to distinguish between different versions of the Brown theory, and a calculation involving no free parameters was discussed in which the two-particle interaction was taken to be a nonsingular potential which fit low-energy nucleon-nucleon scattering data, the results of which were seen to agree with all of the experimental data considered.

The purpose of the present paper is to report the results obtained by applying these same calculations to the case of oxygen 16. The assumptions of the particle-hole theory are expected to be somewhat more valid for this case since this nucleus is doubly magic. It will be seen that very similar results are obtained and substantially the same conclusions may be drawn as in the case of carbon 12. Section II contains a very brief summary of the calculations performed. In Sec. III the numerical results are presented and compared with experiment. Section IV consists of a discussion of the results.

II. CALCULATIONS

The differential cross section for inelastic electron scattering at 180° with excitation of the giant resonance

† This work was supported in part by the U. S. Air Force through the Air Force Office of Scientific Research Grant AF-AFOSR-62-452. Computer time was supported by NSF Grant No. NFS-GP948.

¹ M. Goldhaber and E. Teller, *Phys. Rev.* **74**, 1046 (1948).

² H. Steinwedel and J. H. D. Jensen, *Z. Naturforsch.* **5a**, 413 (1950).

³ W. C. Barber and W. R. Dodge, *Phys. Rev.* **127**, 1746 (1962).

⁴ N. W. Tanner, G. C. Thomas, and E. D. Earle, *Proceedings of the Rutherford Jubilee International Conference, Manchester, 1961*, edited by J. B. Birks (Academic Press Inc., New York, 1961), paper C2/30.

⁵ See for example D. H. Wilkinson, *Physica* **22**, 1039 (1956).

⁶ J. P. Elliott and B. H. Flowers, *Proc. Roy. Soc. (London)* **242A**, 57 (1957).

⁷ G. E. Brown, L. Castillejo, and J. A. Evans, *Nucl. Phys.* **22**, 1 (1961).

⁸ N. Vinh Mau and G. E. Brown, *Nucl. Phys.* **29**, 89 (1962).

⁹ E. Hayward, *Rev. Mod. Phys.* **35**, 324 (1963).

¹⁰ J. Goldemberg, Y. Torizuka, W. C. Barber, and J. D. Walecka, *Nucl. Phys.* **43**, 242 (1963).

¹¹ F. H. Lewis, Jr., J. D. Walecka, J. Goldemberg, and W. C. Barber, *Phys. Rev. Letters* **10**, 493 (1963).

¹² G. R. Bishop and D. B. Isabelle, *Nucl. Phys.* **45**, 209 (1963).

¹³ J. Goldemberg and W. C. Barber (to be published).

¹⁴ F. H. Lewis, Jr., and J. D. Walecka, *Phys. Rev.* **133**, B849 (1964).

is given in first Born approximation, neglecting both nuclear recoil and the electron mass in comparison with its energy, by^{10,11,14}

$$\frac{d\sigma}{d\Omega} = \frac{16\pi\alpha^2 k_2^2}{\Delta^4} |(J=1^- \| T_{1M}^{01}(q) \| J=0^+)|^2,$$

where $\hbar k_2$ is the momentum of the scattered electron, $\hbar q$ and $\hbar\Delta$ are the three- and four-momenta transferred to the nucleus, and α is the fine-structure constant. We refer to the inelastic form factor of the giant resonance as the reduced matrix element of the transverse electric dipole operator between the ground state of O^{16} ($J=0^+$, $T=0$) and the excited state ($J=1^-$, $T=1$). This operator can be written in the form^{10,14,15}

$$T_{1M}^{01}(q) = -\int \frac{1}{q} d\mathbf{x} \{ \mathbf{j}_N(\mathbf{x}) \cdot [\nabla \times j_1(qx) \mathbf{Y}_{111}^M(\Omega_x)] + q^2 \mathbf{u}_N(x) \cdot [j_1(qx) \mathbf{Y}_{111}^M(\Omega_x)] \},$$

where $\mathbf{j}_N(x)$ and $\mathbf{u}_N(x)$ are the nuclear current and magnetization density operators, $j_1(qx)$ are the spherical Bessel functions, and $\mathbf{Y}_{JM}^M(\Omega)$ are the vector spherical harmonics.¹⁵ This operator also describes the absorption and emission of real electric dipole photons by nuclei, but in that case the momentum transfer has only a single fixed value

$$q = q_{fi} = E_{fi}/\hbar c,$$

where E_{fi} is the nuclear excitation energy. The integrated photoabsorption cross section for excitation of the giant resonance is then given by¹⁴

$$\int \sigma_{\text{abs}}(E) dE = (2\pi)^3 \alpha^2 [(\hbar c)^2/E_{fi}] |(1^- \| T_{1M}^{01}(q_{fi}) \| 0^+)|^2.$$

These expressions allow us to obtain the experimental values for the squared inelastic form factor at various values of q from the differential cross sections for electron scattering measured at 180° and various electron energies, and at $q=q_{fi}$ from the total integrated photoabsorption cross section measured for photon energies in the giant resonance region. Note that we do not have to separate the longitudinal and transverse form factors from each other, since only the transverse form factor enters into electron scattering in the backward direction.

The particle-hole theory of the giant resonance and the techniques for calculating the form factors have been discussed extensively elsewhere.^{7,14} In the case of O^{16} we choose as our basis states the five lowest energy shell-model particle-hole states, coupled to $J=1^-$, $T=1$. The configuration energies are chosen from observed energy levels¹⁶ of O^{15} and O^{17} . Using the notation of

¹⁵ A. R. Edmonds, *Angular Momentum in Quantum Mechanics* (Princeton University Press, Princeton, New Jersey, 1957). (We use Edmonds' notation).

¹⁶ T. Lauritsen and F. Ajzenberg-Selove, *Energy Levels of Light Nuclei* (Printing and Publishing Office, National Academy of Sciences—National Research Council, Washington, D. C., 1962).

Ref. 14, we obtain

$$\Phi_{J=1^-, T=1}^{(1d_{3/2})(1p_{3/2})-1};$$

$$E_0((1d_{3/2})(1p_{3/2})^{-1}) = 21.83 + 0.93 = 22.76 \text{ MeV}$$

$$\Phi_{J=1^-, T=1}^{(2s_{1/2})(1p_{3/2})-1};$$

$$E_0((2s_{1/2})(1p_{3/2})^{-1}) = 21.83 - 3.28 = 18.55 \text{ MeV}$$

$$\Phi_{J=1^-, T=1}^{(1d_{5/2})(1p_{3/2})-1};$$

$$E_0((1d_{5/2})(1p_{3/2})^{-1}) = 21.83 - 4.15 = 17.68 \text{ MeV}$$

$$\Phi_{J=1^-, T=1}^{(1d_{3/2})(1p_{1/2})-1};$$

$$E_0((1d_{3/2})(1p_{1/2})^{-1}) = 15.67 + 0.93 = 16.60 \text{ MeV}$$

$$\Phi_{J=1^-, T=1}^{(2s_{1/2})(1p_{1/2})-1};$$

$$E_0((2s_{1/2})(1p_{1/2})^{-1}) = 15.67 - 3.28 = 12.39 \text{ MeV}.$$

The matrix elements of the two-particle interaction $v(1,2)$ (which is the negative of the particle-hole interaction) between these basis states were computed using single-particle wave functions which are eigenfunctions of a particle of mass M (nucleon mass) in a harmonic oscillator potential.¹⁷ The oscillator parameter was chosen by fitting Coulomb energy differences in mirror nuclei.¹⁸ We obtain $b=1.67$ F, where $b=(\hbar/M\omega)^{1/2}$, $\hbar\omega$ =oscillator energy. These wave functions were also used to calculate the matrix elements of $T_{1M}^{01}(q)$ between the ground state and the particle-hole basis states given above, from which the form factors of the diagonalized states were computed.

For the interaction $v(1,2)$ we used two different two-particle potentials and performed the calculations separately for each of these. First we chose $v(1,2)$ to be a Serber force with a Yukawa potential well, with parameters adjusted to fit low-energy nucleon-nucleon scattering data;

$$v(1,2) = [{}^1v(r_{12}){}^1P + {}^3v(r_{12}){}^3P] \left(\frac{1 + P_M(1,2)}{2} \right),$$

where

$${}^1P = \frac{1}{4}(1 - \boldsymbol{\sigma}_1 \cdot \boldsymbol{\sigma}_2), \quad {}^3P = \frac{1}{4}(3 + \boldsymbol{\sigma}_1 \cdot \boldsymbol{\sigma}_2),$$

$P_M(1,2)$ =Majorana exchange operator, $v(r_{12})=(V_0/\mu r)e^{-\mu r}$. The values of the parameters for this force were taken to be¹⁹

$${}^1V_0 = -46.87 \text{ MeV} \quad {}^1\mu = 0.8547 \text{ F}^{-1}$$

$${}^3V_0 = -52.13 \text{ MeV} \quad {}^3\mu = 0.7261 \text{ F}^{-1}.$$

This interaction was also studied in Ref. 14 for the case of carbon 12, and it represents fairly realistically the interaction of two free nucleons at low energy. This interaction has also been shown to give reasonable

¹⁷ P. M. Morse and H. Feshbach, *Methods of Theoretical Physics* (McGraw-Hill Book Company, Inc., New York, 1953), Vols. I and II.

¹⁸ B. C. Carlson and I. Talmi, *Phys. Rev.* **96**, 436 (1954).

TABLE 1. Energy levels and wave functions for the $1^-, T=1$ states in O¹⁶. The Hamiltonian was diagonalized with a Serber force, Yukawa well residual interaction with parameters chosen to fit low-energy nucleon-nucleon scattering data, as discussed in the text.

	$\Phi((1d_{3/2})(1p_{3/2})^{-1})$ $E_0=22.76$ MeV	$\Phi((2s_{1/2})(1p_{3/2})^{-1})$ $E_0=18.55$ MeV	$\Phi((1d_{5/2})(1p_{3/2})^{-1})$ $E_0=17.68$ MeV	$\Phi((1d_{3/2})(1p_{1/2})^{-1})$ $E_0=16.60$ MeV	$\Phi((2s_{1/2})(1p_{1/2})^{-1})$ $E_0=12.39$ MeV
$E_1=26.63$ MeV $\Psi_1:$	0.936	-0.165	-0.072	-0.301	0.012
$E_2=23.89$ MeV $\Psi_2:$	0.214	0.245	0.881	0.322	0.119
$E_3=21.01$ MeV $\Psi_3:$	0.143	0.942	-0.302	0.002	0.030
$E_4=18.65$ MeV $\Psi_4:$	0.238	-0.145	-0.339	0.897	-0.051
$E_5=14.63$ MeV $\Psi_5:$	-0.029	-0.063	-0.113	-0.011	0.991

results for the energy spectra of doubly magic plus two-nucleon nuclei.¹⁹

Our second choice for $v(1,2)$ was an ordinary force with zero range

$$v(1,2) = -v_0\delta(\mathbf{r}_1 - \mathbf{r}_2),$$

similar to the calculations of Ref. 7 and 14. This allowed us to study the sensitivity of our results to the details of the interaction v , and to compare with work done by other authors. The parameter v_0 was chosen to fit the known $T=1, J=1^-$ levels in oxygen 16.¹⁶ For convenience we took $v_0=470$ MeV- F^3 which gives the same value of

$$\lambda = (v_0/b^3) \times 10^{-3} = 0.10 \text{ MeV},$$

as in Ref. 14, and is a few percent less than the value given in Ref. 7.

The form factor was also calculated using the Goldhaber-Teller model; this calculation is completely analogous to the calculations described in Ref. 10. The elastic scattering form factor²⁰ of O¹⁶ is taken from tables in Ref. 20 for the uniform model with $a_u=2.64$ F.

III. NUMERICAL RESULTS AND COMPARISON WITH EXPERIMENT

In this section we will present the numerical results of the theoretical calculations and compare them with the experimental data. We will first discuss the particle-hole calculation using the Serber force, Yukawa well interaction; this calculation is significant in that the particle-hole interaction resembles approximately the interaction between two free particles, and the results are in remarkable agreement with experiment. Secondly, we will discuss the results of the ordinary zero-range force calculations similar to those of Brown *et al.*⁷ The Goldhaber-Teller model has been discussed in Ref. 10,

¹⁹ J. F. Dawson, I. Talmi, and J. D. Walecka, Ann. Phys. (N. Y.) **18**, 339 (1962), Table VI.

²⁰ R. Herman and R. Hofstadter, *High-Energy Electron Scattering Tables* (Stanford University Press, Stanford, California, 1960), p. 116.

and we will simply indicate the results for this calculation.

The matrix elements between the particle-hole basis states were computed using a residual interaction $v(1,2)$ which was a Serber force, Yukawa well with parameters adjusted to fit low-energy nucleon-nucleon scattering data as discussed in Sec. II. The 5×5 Hamiltonian matrix was then constructed and diagonalized with the aid of the IBM 7090 computer at the Stanford University Computation Center. The resulting eigenvalues and eigenstates are given in Table I.

The giant resonance in oxygen 16 appears both in photoabsorption and ground-state proton capture [i.e., (p,γ_0) reaction] experiments^{4,9,21} and in electron-scattering data¹³ as a broad region of excitation energies roughly between 20 and 27 MeV in which the cross section for electromagnetic excitation is large and contains considerable structure. From Table I we see that the theory predicts that there are three states lying in the energy range of 20–27 MeV, which are denoted by Ψ_1, Ψ_2 , and Ψ_3 . We will therefore interpret the observed cross sections in terms of these three states alone. We are assuming here that practically all of the transition strength observed in electron scattering as well as in photoabsorption and (p,γ_0) experiments arises from $E1$ transitions. As was mentioned in Ref. 14, the single-particle Weisskopf estimates for $M1, E2$, and $M2$ transitions in electron scattering at $q=120$ MeV/ c and $E_{fi}=20$ MeV are $\sim 10\%$ of the observed cross sections for the giant resonance.¹³

We calculate the sum of the squares of the form factors $|(J=1^-, T=1||T_1^{el}(q)||J=0^+, T=0)|^2$ for the states Ψ_1, Ψ_2 , and Ψ_3 ; this sum we interpret as the squared form factor of the giant resonance, and it is plotted as a function of q in Fig. 1 (solid curve). The 180° electron scattering cross sections have been measured by Goldemberg and Barber¹³ in oxygen 16 for incident electron energies of 54 and 70 MeV; using

²¹ E. G. Fuller and E. Hayward, in *Nuclear Reactions*, edited by P. M. Endt and P. B. Smith (North-Holland Publishing Company, Amsterdam, 1962), Vol. II, p. 113.

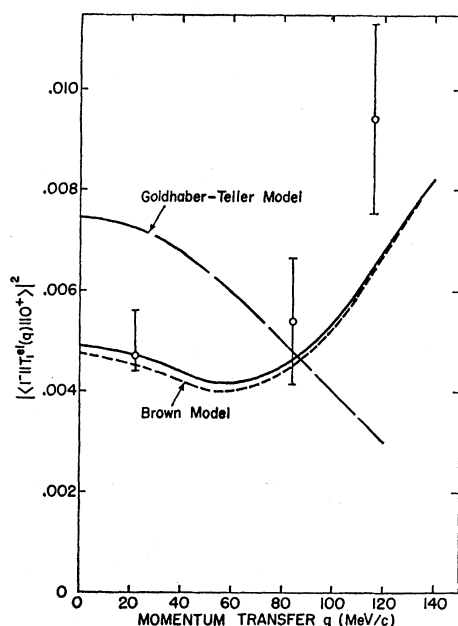


Fig. 1. Squared form factor versus momentum transfer for the giant dipole resonance in oxygen 16. The solid curve is calculated using a Serber force with a Yukawa potential well for the residual interaction, while the short-dash curve is calculated using an ordinary force with zero range. The long-dash curve using the Goldhaber-Teller model is also indicated. The experimental points shown are discussed in the text.

these cross sections we have calculated the squared form factors of the giant resonance at momentum transfers of 84 MeV/c and 116 MeV/c (we have used a "mean excitation energy" of 24 MeV in the kinematical calculations). These squared form factors are also plotted in Fig. 1.

Finally we have used the photoabsorption data of Burgov *et al.*²² to obtain the squared form factor at a momentum transfer of 22 MeV/c; this form factor is also indicated in Fig. 1. Note that we have used a slightly higher excitation energy for the electron-scattering form factors than for the photoabsorption form factor in order to compensate for the observed shift of the transition strength to higher energy as the momentum transfer is increased. The numerical value of this form factor and the error bars shown for this point are calculated directly from the values for $\int \sigma(E)dE$ reported in Ref. 22. This particular reference was used because the experimental method involves a direct measurement of the total integrated photoabsorption cross section independently of the decay modes of the giant resonance. The results are consistent with those obtained by other authors.^{4,9,21}

We wish to call attention to the fact that the experimental measurements of the squared form factor of the giant resonance are clearly consistent with the

²² N. A. Burgov, G. V. Danilyan, B. S. Dolbilkin, L. E. Lazareva, and F. A. Nikolaev, Zh. Eksperim. i Teor. Fiz. 43, 70 (1962) [English transl.: Soviet Phys.—JETP 16, 50 (1963)].

theoretical predictions of the particle-hole theory as shown in Fig. 1. Note that the theory predicts that there is a dip in the squared form factor; this dip arises because the giant resonance is made up of the three states Ψ_1 , Ψ_2 , and Ψ_3 . As the momentum transfer q increases the squared form factors of Ψ_1 and Ψ_3 increase while that of Ψ_2 decreases; the sum therefore goes through a minimum.

This effect can also be clearly seen by looking at Fig. 2, where we have shown the squared form factors (or relative transition strengths) for all five states at several different values of momentum transfer q . (These are labeled Serber Force, Yukawa Well). The theory predicts that for low-momentum transfers there is a maximum in the cross section as a function of energy and that as q increases this maximum shifts to higher energy by about 3 MeV. The theory also predicts that at low values of q the transition strength at 21 MeV is very small, and that as q increases this transition strength increases, relative to the transition strength in the region around 24 MeV, for example.

These predictions are to be compared with the experimental results which are shown in Fig. 3. The central graph contains the experimental photoabsorption data of Burgov *et al.*²² The upper graph shows schematically the predictions of the calculation of Elliott and Flowers⁶ for the zero momentum-transfer case, where a width of

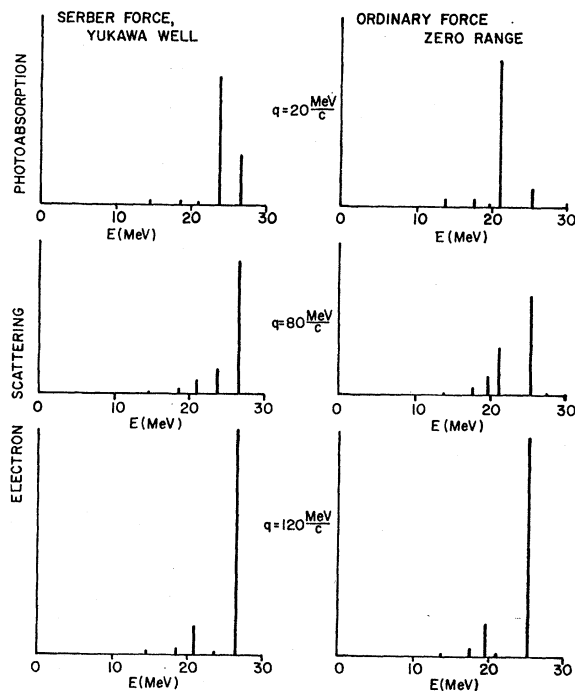


Fig. 2. Relative transition probabilities for transverse excitation of the $1^-, T=1$ states in oxygen 16. The length of each line is proportional to the square of the form factor for excitation of the corresponding state at the given energy and momentum transfer. The two types of residual interaction indicated are discussed in the text.

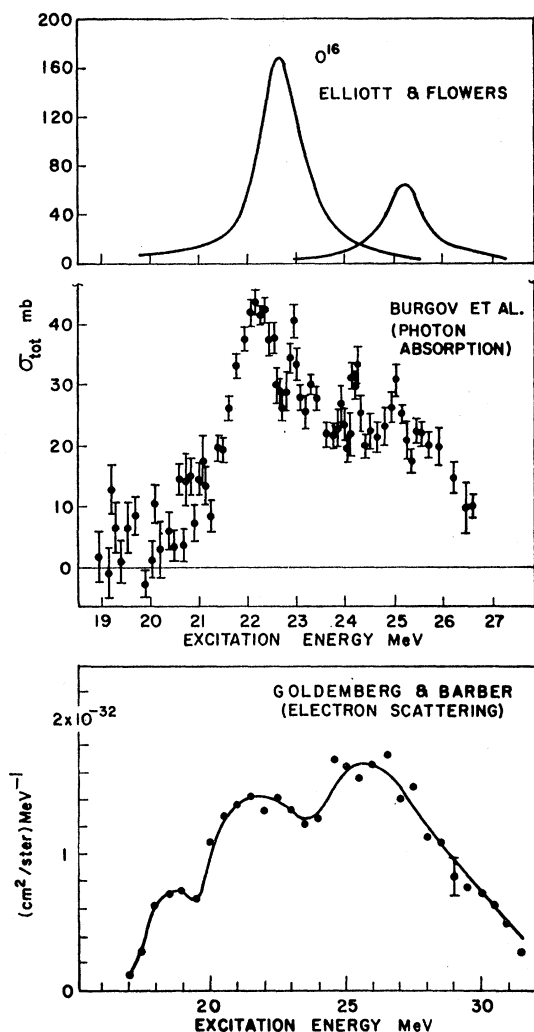


FIG. 3. A comparison of the photon absorption cross section measurements of Burgov *et al.*²² in oxygen 16 with the 180° electron-scattering cross section measurements of Goldemberg and Barber¹³ using incident electrons of 70-MeV energy. The top graph shows schematically the results of the calculation of Elliott and Flowers.⁶

1 MeV has been arbitrarily assigned to each of the two states shown. These two graphs are taken directly from Fig. 7 of Ref. 9. The lower graph shows the 180° electron scattering data of Goldemberg and Barber¹³ for an incident electron energy of 70 MeV, i.e., a momentum transfer of $q=116$ MeV/ c . Figure 3 is also shown and discussed in Ref. 13.

By comparing the photoabsorption data with the electron scattering data in Fig. 3 one sees clearly that as q increases from 22 to 116 MeV/ c there is a maximum in the cross section which shifts upward in energy by about 3 MeV, and that the cross section at 21 MeV is relatively small for the photoabsorption data but develops a sizable bump in the electron scattering data. We see that the predictions of the theory concerning the change in the structure of the giant resonance as a

function of q are confirmed experimentally. Again, these results occur because the giant resonance is composed of 3 states, and as q increases there is a shift of transition strength from Ψ_2 to Ψ_1 and Ψ_3 .

The spectrum of oxygen 16 also contains two other 1^- , $T=1$ states¹⁶ observed at 17.3 and 13.1 MeV. We describe these two states by the wave functions Ψ_4 and Ψ_5 , respectively. The calculated energies of these states are within 1.6 MeV of the experimental levels. The squared inelastic form factors for excitations of these states have been plotted as functions of q in Figs. 4 and 5. The total integrated photoabsorption cross sections for various intervals of excitation energies in oxygen 16 have been given in the review article of Fuller and Hayward²¹ (Table 11). By making the usual assumption that in the limit of long wavelengths the 1^- , $T=1$ states carry practically all of the transition strength, we have used their results to obtain squared form factors for the 17.3-MeV state and the 13.1-MeV state at momentum transfers corresponding to photoexcitation. These experimental form factors are also shown in Figs. 4 and 5. The error bars on these points represent typical experimental errors.

For larger values of q one finds that it is quite difficult to obtain experimental form factors for these states from the electron scattering experiments. This is primarily because at larger values of q one can excite states other than 1^- , $T=1$ states with appreciable transition probabilities. In comparison with the electron scattering Weisskopf estimates for $M1$ and $E2$ transitions mentioned earlier, the predicted cross sections for the 17.3- and 13.1-MeV states are fairly small. If one considers the 180° electron scattering data of Ref. 13 one finds that there is considerable structure in the cross section between 12 and 20 MeV which is quite difficult to identify in any unambiguous way with the excitation of the states at 17.3 and 13.1 MeV. If one

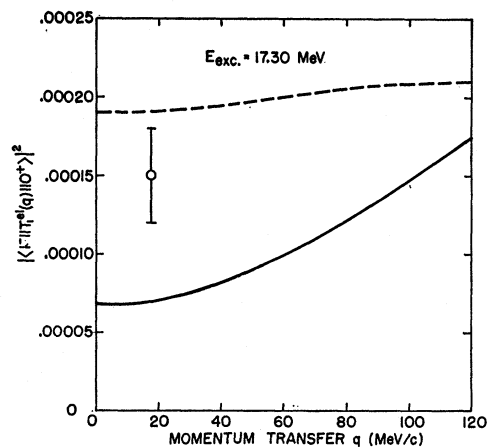


FIG. 4. Squared form factor versus momentum transfer for the 1^- , $T=1$ state at 17.3 MeV in oxygen 16. The solid curve is calculated using a Serber force, Yukawa well and the dashed curve is calculated using an ordinary force, zero range. The experimental point shown is discussed in the text.

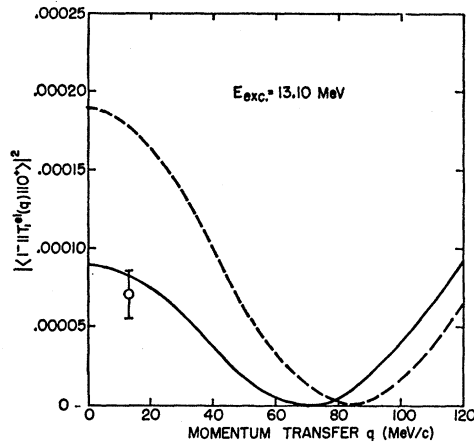


FIG. 5. Squared form factor versus momentum transfer for the 1^- , $T=1$ state at 13.1 MeV in oxygen 16. The solid curve is calculated using a Serber force, Yukawa well and the dashed curve is calculated using an ordinary force, zero range. The experimental point shown is discussed in the text.

uses the observed cross section at ~ 17 or ~ 13 MeV to calculate a squared form factor, assuming that the cross section arises solely from excitation of a single state, one obtains results which are four or five times larger than the values predicted by the theory, shown in Figs. 4 and 5.

We are thus led to conclude that the structure of the cross sections observed in electron scattering around 13 and 17 MeV is not due only to excitation of the 1^- , $T=1$ states, but that instead one is observing primarily transitions of different multiplicities. Although in the photoabsorption and (p,γ) experiments one observes only the electric dipole transitions due to the low-momentum transfers, the importance of other transitions in electron scattering has been pointed out by Willey,²³ who has calculated both longitudinal and transverse form factors on the basis of the particle-hole theory for various excited states in O^{16} and compared the results with the electron-scattering data of Isabelle and Bishop.^{12,24} Willey has shown that one may also easily observe 2^- and 3^- as well as 1^- , $T=1$ states at about 13 MeV in electron scattering, and that the strongly excited levels observed in electron scattering¹² at about 19 MeV have a transition strength essentially in agreement with the theoretical calculation for the sum of the cross sections of 1^- , 2^- , and 3^- , $T=1$ states lying near this energy region. (Note that some evidence for the strength of these excitations also appears to be present in the 180° electron-scattering data,¹³ as shown in Fig. 3, for example.) While such results hold for somewhat higher values of q than we are considering here, and also include effects from the longitudinal form factor, they serve to indicate how states other than 1^- , $T=1$ states can be important in electron scattering at energies outside the giant resonance region.

²³ R. S. Willey, Phys. Letters 6, 336 (1963).

²⁴ G. R. Bishop and D. B. Isabelle, Phys. Letters 1, 323 (1963).

We have repeated the particle-hole calculations described above using for the residual interaction $v(1,2)$ an ordinary force with zero range, discussed in Sec. II. This is essentially the same calculation as that done by Brown, Castillejo, and Evans,⁷ and our numerical results are almost exactly the same as those reported by these authors. In addition, we have calculated the squared inelastic transverse form factors of the five diagonalized states in the same way as done previously. Choosing again the sum of the squares of the form factors for the three highest energy states predicted at 25.5, 21.4, and 19.9 MeV to be the squared form factor of the giant resonance, we have plotted this quantity as a function of q in Fig. 1 (shown by the dotted curve labeled "Brown model"). We have also shown the squared form factor which one obtains from the Goldhaber-Teller model of the giant resonance.^{1,10} We see that both of the particle-hole calculations give very similar form factors which are in agreement with experiment, while the collective motion model of Goldhaber and Teller gives a completely different form factor which disagrees with experiment.

In Fig. 2 we have shown the relative transition strengths (squared form factors) at various values of q for all five states obtained in the zero-range force calculation. One finds that the distribution of dipole strength is qualitatively similar for the two different particle-hole calculations.

Figures 4 and 5 indicate the squared form factors of the two lower energy states calculated at 17.7 and 13.8 MeV which we interpret as the observed states at 17.3 and 13.1 MeV, respectively. (These form factors are represented by the dotted curves.) We find that in comparing the form factors for small q with the experimental form factors from photoabsorption experiments the zero-range force calculation gives slightly better agreement for the 17.3-MeV state and considerably worse agreement for the 13.1-MeV state. However, one should not take these results too seriously since we are here only comparing absolute cross sections at one

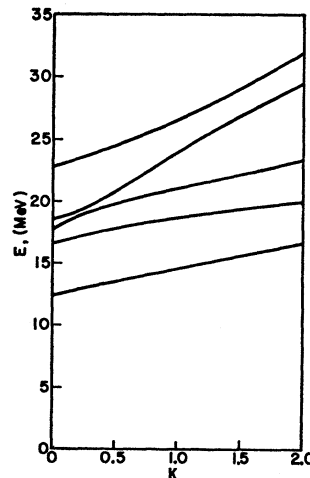


FIG. 6. Energy levels of the 1^- , $T=1$ states in oxygen 16 as a function of the residual interaction strength. The interaction used was a Serber force with a Yukawa potential well. The quantity κ is the fraction of the free particle interaction strength.

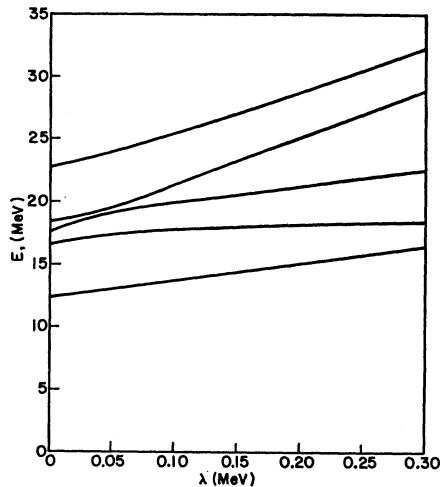


FIG. 7. Energy levels of the $1^-, T=1$ states in oxygen 16 as a function of the residual interaction strength. The interaction used was an ordinary force with zero range. The parameter λ is discussed in the text.

point, whereas we have seen that the really conclusive results come from comparing the behavior of the form factors as a function of q .

Finally, we have considered the behavior of the energy levels of the five states as a function of the strength of the residual interaction for the particle-hole calculations. For the case where the interaction $v(1,2)$ was a Serber force, Yukawa well with parameters chosen to fit low-energy nucleon-nucleon scattering, we replaced $v(1,2)$ by $\kappa v(1,2)$ and, allowing κ to vary over a range of values, we calculated the energies of the five eigenstates of the Hamiltonian matrix. The resulting energy levels are shown as functions of κ in Fig. 6. Similarly, for the case where $v(1,2)$ is an ordinary force with zero range, we calculated the energies of the five states as functions of λ , defined in Sec. II. These are shown in Fig. 7.

Let us re-emphasize here the point made in Ref. 14 that the value $\lambda=0.10$ MeV for the zero-range force, used both here and in Ref. 14 to calculate form factors, which approximately fits the observed energy levels in O¹⁶ and C¹² of the $1^- T=1$ states and which is close to the value used in Refs. 7 and 8, yields a volume integral of the potential which is two to three times smaller than one obtains using potentials with parameters chosen to fit low-energy nucleon-nucleon scattering data. In contrast to this, the value of $\kappa=1$ for the interaction strength of the Serber force which is equal to the *full* interaction strength for free nucleons, yields energy levels which are approximately in agreement with experiment. It was shown in Ref. 14 that this result is independent of the detailed shape of the potential well.

IV. DISCUSSION

The calculations reported in this paper are all very similar to the work discussed in Ref. 14 for the case of

carbon 12. The particle-hole theory of the giant resonance has been applied to the case of oxygen 16 using for the residual interaction $v(1,2)$ a nonsingular potential with parameters adjusted to fit low-energy nucleon-nucleon scattering data. Thus there are no free parameters in the calculation; all of the input data are taken from other experiments. The results are used to calculate the transverse inelastic form factors for excitation of the giant resonance, and comparison is made with photoabsorption and (p,γ) data and with the 180° electron scattering experiments.

There are two main points which we want to make as a consequence of these calculations:

(1) The detailed comparison which can be made between theory and experiment concerning the structure of the giant resonance illustrates once more the fact that electron scattering can yield an enormous amount of valuable information about nuclear structure.

(2) The particle-hole description of the giant resonance in oxygen 16 is in quite good quantitative agreement with the experimental results for transverse electromagnetic excitations.

The results for the squared form factor of the giant resonance of O¹⁶ shown in Fig. 1 are very similar to the corresponding results for C¹² (Ref. 14). The particle-hole theory again predicts a dip, which is consistent with experiment, while the Goldhaber-Teller collective model completely fails to produce the right behavior. The reasons for the occurrence of this dip are much the same for oxygen 16 as for carbon 12, since the particle-hole states involved are similar for the two cases.

Comparison of Figs. 2 and 3 indicates clearly that the qualitative behavior of the shape of the giant resonance as a function of q predicted by the particle-hole theory is observed in the experimental data. One should not try to make too quantitative a comparison here because the theoretical calculations included no mechanism for the width of the states involved and the quantities shown in Fig. 2 represent total areas under a given experimental peak. The experiments show, however, that the states involved have large overlapping widths which are not in general well known. Fig. 2 should therefore be regarded as a general indication of the over-all shape of the giant resonance cross section.

Calculations similar to those of Brown *et al.*⁷ using a residual interaction with zero-range yield a form factor for the giant resonance which is quite similar to the form factor obtained using a Serber force with parameters chosen to fit low-energy nucleon-nucleon scattering data. The form factors for the two lower energy states are somewhat different in absolute magnitude for the two theories, although they are similar in shape as seen in Figs. 4 and 5.

The most remarkable distinction between these two

calculations, however, occurs in the prediction of the energy levels of the different states. The Serber force calculation gives energy spectra of the 1^- , $T=1$ states in essential agreement with experiment using a strength parameter equal to that for the free nucleon-nucleon interaction. On the other hand for the zero-range force we must use an interaction strength two to three times smaller than the free-particle strength in order to obtain reasonable agreement with the experimental spectrum of oxygen 16. As shown in Ref. 14, this weakening of the interaction is obtained mainly by using the Serber exchange-force mixture, which has no contribution in relative odd angular-momentum states.

ACKNOWLEDGMENTS

I wish to express my gratitude to Dr. John D. Walecka for his patient guidance, enthusiastic encouragement, and critical discussions, which were of invaluable help during the course of this work. I am grateful to Dr. J. Goldemberg for stimulating discussions about this problem, for his help in analyzing the experimental results, and for making available to me experimental data before publication. I am indebted to Dr. L. I. Schiff for his reading and helpful criticism of the manuscript. Finally I wish to thank Dr. W. Czyz for many interesting discussions.

Studies of Electromagnetic Transitions in N^{14} by Means of the $C^{12}(He^3, p)N^{14}$ Reaction*

E. K. WARBURTON, J. W. OLNESS, D. E. ALBURGER, D. J. BREDIN, AND L. F. CHASE, JR.†
Brookhaven National Laboratory, Upton, New York

(Received 4 December 1963)

The electromagnetic decays of the N^{14} states between 5 and 6.5 MeV were studied using the $C^{12}(He^3, p)N^{14}$ reaction. From investigations of the gamma-ray spectra on and off the 3.0-MeV resonance for production of the N^{14} 6.44-MeV level, this state was found to decay to the ground, 3.95-, and 5.10-MeV levels of N^{14} with branching ratios of $(65\pm 3\%)$, $(21\pm 2\%)$, $(14\pm 3\%)$, respectively. From a study of the internal pairs corresponding to the 6.21 \rightarrow 2.31 transition, this transition was shown to be predominantly $M1$ so that the N^{14} 6.21-MeV level has even parity. Similarly, it was confirmed that the N^{14} 6.44 \rightarrow 0 transition is predominantly $E2$. The angular distributions of the gamma rays from $C^{12}+He^3$ at $E_{He^3}=2.75$ MeV were measured. It was shown that the mixing parameter x (amplitude ratio of quadrupole to dipole radiation) for the 5.69 \rightarrow 0 transition is $x=+0.03\pm 0.03$ and for the 5.10 \rightarrow 0 transition $x=-0.12\pm 0.03$. The branching ratios of the N^{14} 5.10-, 5.69-, and 6.21-MeV levels to the N^{14} ground state and 2.31-MeV first excited state were measured. The results are in satisfactory agreement with previous determinations.

I. INTRODUCTION

ELECTROMAGNETIC transitions in N^{14} have recently been investigated at this laboratory using the $C^{13}(d, n)N^{14}$ reaction.^{1,2} It was found that at the deuteron energies used (1.9–3.1 MeV) the N^{14} 6.21-MeV level was excited quite weakly, so that the gamma rays from the decay of this state were not observed. The ground-state transition from the N^{14} 6.44-MeV level was observed, but the state was excited so weakly as to make it difficult to study transitions from this level via the $C^{13}(d, n)N^{14}$ reaction.

Recent work at Rice³ has shown that the 6.21- and 6.44-MeV levels of N^{14} are produced in the $C^{12}(He^3, p)N^{14}$

reaction, at a bombarding energy of 3 MeV, with cross sections comparable to those of the lower excited states of N^{14} . There is, in fact, a strong resonance with a laboratory width $\Gamma=(125\pm 10)$ keV for the production of the 6.44-MeV level (but not the 6.21-MeV level) at $E_{He^3}=2.99$ MeV³, and the presence of this resonance greatly facilitates a study of the electromagnetic transitions from the 6.44-MeV level. Furthermore, the only gamma rays with energies greater than 2.5 MeV which are expected from $C^{12}+He^3$ at 3-MeV bombarding energy are those from the $C^{12}(He^3, p)N^{14}$ reaction ($Q=4.77$ MeV). This lack of competing reactions is in contrast to a study of N^{14} transitions via $C^{13}+d$ where interfering radiations arise from the $C^{13}(d, p)C^{14}$ reaction.

One purpose of this investigation, then, was to study the electromagnetic transitions from the decay of the N^{14} levels at 6.21 and 6.44 MeV. For the former level the decay modes are known and our aim was to determine the parity of this level which was not definitely established when this work was started.⁴ For the

* Work performed under the auspices of the U. S. Atomic Energy Commission.

† Permanent address: Lockheed Missiles and Space Laboratory, Palo Alto, California.

¹ D. E. Alburger and E. K. Warburton, Phys. Rev. **132**, 790 (1963).

² E. K. Warburton, D. E. Alburger, A. Gallmann, P. Wagner, and L. F. Chase, Jr., Phys. Rev. **133**, B42 (1964).

³ H. Kuan, T. A. Belote, J. R. Risser, and T. W. Bonner, Bull. Am. Phys. Soc. **8**, 125 (1963); and H. Kuan (private communication).

⁴ F. Aijzenberg-Selove and T. Lauritsen, Nucl. Phys. **11**, 1 (1959).